Articles

Synthesis and Structural Characterization of the First Organically Templated Vanadyl(IV) Arsenato- and Phosphato-oxalates: $(C_4H_{12}N_2)[VO(C_2O_4)HXO_4]$ (X = As, P)

Yu-Min Tsai,[†] Sue-Lein Wang,*[,†] Ching-Hui Huang,[‡] and Kwang-Hwa Lii[‡]

Department of Chemistry, National Tsing Hua University, Hsinchu, Taiwan 300, and Department of Chemistry, National Central University, Chungli, Taiwan 320

Received May 10, 1999

Two novel piperazinium vanadyl(IV) compounds, $(C_4H_{12}N_2)[VO(C_2O_4)HAsO_4]$ (**1**) and $(C_4H_{12}N_2)[VO(C_2O_4)HPO_4]$ (**2**), have been prepared under mild hydrothermal conditions and structurally characterized by single-crystal X-ray diffraction, thermogravimetric analysis, and magnetic susceptibility. They adopt a one-dimensional structure in which ladder-like chains are constituted by the three-connected V and three-connected X (X = As for **1** and P for **2**) centers. Within the infinite chains the oxalate group coordinates to each of the V centers as a bidentate ligand. They are the first inorganic/organic mixed-anion materials prepared in the vanadium arsenate and vanadium phosphate systems. Crystal data for **1**: orthorhombic, $P2_12_12_1$, $a = 6.5595(1)$ Å, $b = 12.4689(1)$ Å, $c = 14.6363(1)$ Å, $Z = 4$. Crystal data for **2**: as above, except $a = 6.4022(4)$ Å, $b = 12.4735(8)$ Å, $c = 14.653(1)$ Å. Acccording to the results of TG analysis, both compounds are thermally stable to *ca*. 250 °C. Our magnetic study revealed that exchange coupling occurred between the nearest VO^{2+} centers along the infinite $(-V-O-X-O)_2$ chains. Good fits of the magnetic susceptibility data were obtained by using the Bonner and Fisher $S = {}^1/_2$ linear chain model.

Introduction

Hydrothermal crystallization, in the presence of organic templating agents, has provided a convenient route to microporous tetrahedral framework solids, such as zeolites and alumino-phosphates.[1] More recently, it has become a versatile technique for the preparation of a variety of open-framework transition metal phosphates.[2] For example, the chiral double-helix-like vanadyl(IV) compound, $[(CH_3)_2NH_2]K_4[V_{10}O_{10}(H_2O)_2(OH)_4(PO_4)_7]\cdot 4H_2O$,[3] contains enormous cavities and the novel structure of the iron(III) phosphate, $[H_3N(CH_2)_3NH_3]_2[Fe_4(OH)_3(HPO_4)_2(PO_4)_3]\cdot xH_2O$,[4] possesses large tunnels with 20-ring windows. In these structures, the cationic organic amine is occluded within an anionic inorganic framework. Recent reports indicate that microporous structures can be prepared by exploiting appropriate metal centers linked through suitable multidentate organic ligands.[5] This approach makes possible the rational design and synthesis of coordination polymers with potential interesting properties. To combine the robustness of the inorganic framework with the greater chemical flexibility of the organic ligand, we incorporated both inorganic and organic anions into the structure to provided a new route to open−framework materials and successfully prepared two iron phosphatooxalates with intersecting tunnel structures.[6] According to our literature search, the two iron compounds, $(C_4H_{12}N_2)[Fe_4(C_2O_4)_3(HPO_4)_2]$ and $(C_4H_{12}N_2)[Fe_2(C_2O_4)(HPO_4)_3]$, reported by us and the compound $Fe_4(PO_4)_2(C_2O_4)(H_2O)_2$ reported by others[7] have been the only structurally characterized transition-metal phosphatooxalates.[8] To exploit more possibilities, we have extended our investigations into the vanadium metal phosphate and arsenate systems. We report *herein* the first metal arsenatooxalate, $(C_4H_{12}N_2)[VO(C_2O_4)HAsO4]$ (**1**), and the first vanadium phosphatooxalate, $(C_4H_{12}N_2)[VO(C_2O_4)HPO_4]$ (**2**). Both contain the ladder-like $(-V-O-X-O)_2$ (X = As, P) chains with

[†] National Tsing Hua University.
[‡] National Central University.

(1) (a) Occelli, M. L.; Robson, H. E. *Zeolite Sunthesi;* American Chemical Society; Washington, DC, 1989. (b) Barrer, R. M. *Hydrothermal Chemistry of Zeolites*; Academic Press: New York, 1982.
(2) (a) Lii, K. H.; Huang, Y. F.; Zima, V.; Huang, C. Y.; Lin, H. M.; Jiang, Y. C.; Liao, F. L.; Wang, S. L. *Chem. Mater*. **1998**, *10*, 2599. (b) Lii, K. H.; Huang, Y. F. *Inorg. Chem*. **1999**, *38*, 1348. (c) Huang, C. Y.; Wang, S. L.; Lii, K. H. *J. Porous Mater*. **1998**, *5*, 147. (d) Lin, H. M.; Lii, K. H. *Inorg. Chem.* **1998**, *37*, 4220. (e) Zima, V.; Lii, K. H.; Nguyen, N.; Ducouret, A. *Chem. Mater*. **1998**, *10*, 1914. (f) Lii, K. H.; Huang, Y. F. *Chem. Commun.* **1997**, *14*, 1311.
(3) Soghomonian, V.; Chen, Q.; Haushalter, R. C.; Zubieta, J.; O'Connor, C. J. *Science* **1993**, *259*, 1596.
(4) Lii, K. H.; Huang, Y. F. *Chem. Commun.* **1997**, *9*, 839.
(5) (a) Yaghi, O. M.; Li, G.; Li, H. *Nature* **1995**, *378*, 703. (b) Gutsshke, S. O. H.: Molinier, M.; Powell, A. K.; Winpenny, R. E. P.; Wood, P. T. *J. Chem. Soc., Chem. Commun*. **1996**, 823. (c) Abrahams, B. F.; Hoskins, B. F.; Michail, D. M.; Robson, R. *Nature* **1994**, 369, 727. (d) Macgillivray, L. R.; Subramanian, S.; Zaworotko, M. J. *J. Chem. Soc., Chem. Commun*. **1994**, 1325.
(6) Lin, H. M.; Lii, K. H.; Jiang, Y. C.; Wang, S. L. *Chem. Mater*. **1999**, *11*, 519.
(7) Lethbridge, Z.; Lightfoot, P. *J. Solid State Chem*. **1999**, *143*, 58.
(8) There are three nontransition metal phosphato-oxalates which have been reported, see: (a) Huang, Y. F.; Lii, K. H. J. *Chem. Soc., Dalton Trans*. **1998**, 4085. (b) Natarajan, S. *J. Solid State Chem*. **1998**, *139*, 200. (c) Lightfoot, P.; Lethbridge, Z.; Morris, R. E.; Wragg, D. S.; Wright, P. A. *J. Solid State Chem*. **1999**, *143*, 74.

10.1021/ic990501p CCC: $18.00
Published on Web 08/31/1999

Table 1. Crystallographic Data for **1** and **2**

	1	**2**
empirical formula	$C_6H_{13}AsN_2O_9V$	$C_6H_{13}PN_2O_9V$
fw	383.04	339.09
space group	$P2_12_12_1$	$P2_12_12_1$
a, Å	6.5595(2)	6.4022(4)
b, Å	12.4689(1)	12.4735(8)
c, Å	14.6363(3)	14.653(1)
volume, Å^3	1197.10(3)	1170.2(1)
Z	4	4
D_{cacl}, gcm^{-3}	2.125	1.925
μ, mm^{-1}	3.618	1.032
T, °C	22	22
λ, Å	0.710 73	0.710 73
R1[a]	0.0333	0.0390
wR2[b]	0.0793	0.0807

[a] $R1 = \sum||F_o| - |F_c||/\sum|F_o|$. [b] $wR2 = [\sum w(|F_o|^2 - |F_c|^2)^2]/\sum w(|F_o|^2)^2]^{1/2}$, $w = [\sigma^2(F_o^2) + 0.0431P]^2 + 1.8491P]$ for **1**, and $w = [\sigma^2(F_o^2) + 0.0294P]^2 + 1.1714P]$ for **2**, where $P = (F_o^2 + 2F_c^2)/3$.

the same topology as that in $VO(HPO_4)\cdot 4H_2O$.[9] The infinite chains can be considered as derived from the layers of the well-known structure of $VOPO_4\cdot 2H_2O$.[10] In this paper, the synthesis, crystal structure, TG analysis, and magnetic susceptibility of the title compounds are presented.

Experimental Section

Synthesis. Chemicals of reagent grade or better were used as received, and all reactions were carried out in Teflon-lined digestion bombs with an internal volume of 23 mL under autogenous pressure by heating the reaction mixtures at 160 °C for 3 days followed by slow cooling at 5 °C h^{-1} to room temperature. Compound **1** was prepared from a reaction mixture of piperazine (3.0 mmol), VO_2 (3.0 mmol), H_3AsO_4 (3.0 mmol dm^{-3}), $H_2C_2O_4\cdot 2H_2O$ (3.0 mmol), and 12.0 mL of water. The product contains green columnar crystals of **1** as a major phase and a small amount of unknown black material. Compound **2** was prepared from a reaction solution of piperazine (4.0 mmol), VO_2 (3.0 mmol), H_3PO_4 (3.6 mmol dm^{-3}), $H_2C_2O_4\cdot 2H_2O$ (3.0 mmol), and 10.4 mL of water. The product contained a large portion of green columnar crystals of **2**, a small quantity of transparent crystals of ammonium phosphate, and unknown black powders. Attempts to prepare single phases for both compounds have not been successful. The samples used for the following chemical and physical measurements were hence from manually selected crystals of which the powder X-ray diffraction patterns agreed well with those calculated from single-crystal data (see below).

Elemental analysis confirmed the amount of piperazine in both compounds according to the formula proposed. Found for **1**: C, 18.76; N, 7.24; H, 3.58. Calcd: C, 18.81; N, 7.31; H, 3.42. Found for **2**: C, 20.85; N, 8.06; H, 3.66. Calcd: C, 21.25; N, 8.26; H, 3.86. Thermogravimetric analyses (TGA), using a Du Pont 951 thermal analyzer, were performed on powder samples in flowing N2 with a heating rate of 10 °C min^{-1}. A 10.3 mg sample of compound **1** and 38.6 mg of compound **2** were used to collect variable temperature magnetic susceptibility $\chi(T)$ data from 2 to 300 K in a magnetic field of 5 kG using a Quantum Design SQUID magnetometer. The measured susceptibility data were corrected for core diamagnetism.[11]

Single-Crystal X-ray Structure Analysis. Crystal structures of both compounds **1** and **2** were determined by single-crystal X-ray diffraction methods. Crystallographic data are listed in Table 1. The procedures for **1** are given in the following. A columnar crystal of dimensions 0.05 × 0.05 × 0.20 mm was used for indexing and intensity data collection on a Siemens Smart-CCD diffractometer equipped with a normal focus, 3 kW sealed-tube X-ray source (λ = 0.710 73 Å). Intensity data were collected in 1271 frames with increasing ω (width of 0.3° per frame). Unit cell dimensions were determined by a least-squares fit of 5129 reflections. The intensity data was corrected for *Lp* and absorption effects. Number of measured and observed reflections ($I_{obs} > 3\sigma_I$) are 7119 and 6355, respectively. The absorption correction was based on symmetry−equivalent reflections using SADABS program.[12] On the basis of systematic absences and statistics of intensity distribution, the space group was determined to be $P2_12_12_1$. The structure was solved by direct methods, the vanadium, arsenic, and a few oxygen atoms with the remaining non-hydrogen atoms being found from successive difference maps. The results of bond valence sum calculations[13] were used to identify the hydroxo oxygen atom, O(4). All of the hydrogen atoms were directly located from Fourier difference maps calculated at the final stage of structure refinements. The final cycle of refinement, including the atomic coordinates and anisotropic thermal parameters for all non-hydrogen atoms and fixed atomic coordinates and isotropic thermal parameters for the hydrogen atoms, converged at R1 = 0.033 and wR2 = 0.079 for 2147 unique reflections. Corrections for secondary extinction and anomalous dispersion were applied. Neutral−atom scattering factors for all atoms were taken from the standard sources. All calculations were performed by using SHELXTL programs.[14]

Additional crystallographic results are given in the Supporting Information.

Results and Discussion

The atomic coordinates and the bond lengths and bond valence sums[13] of the title compounds are given in Tables2 and 3, respectively. Bond valence calculations clearly indicate that the compounds are vanadium(IV) species. As depicted in Figure 1, the V center is coordinated by a terminal oxo group, O(5), three oxygen atoms from three $HAsO_4^{2-}$ groups, and two oxygen donors from the bidentate oxalate group. The As center is coordinated by a terminal hydroxo group, O(4)H, and three μ_2-O atoms shared with different V centers. The connectivity results in a ladder-like (-V-O-As-O)$_2$ chain running parallel to the *a* axis (see Figure 2). A similar chain exists in the structure of $VOHPO_4\cdot 4H_2O$.[9] The title compounds can be considered as derivatives of $VOHPO_4\cdot 4H_2O$ (in better formulation as $VO(H_2O)_2(HPO_4)\cdot 2H_2O$), i.e., one oxalate anion replaces two coordination water molecules and one piperazinium cation replaces two lattice water molecules.

The oxalate anion participates in strong H bonds which play an important role in the connections among anionic chains in the structure. As shown in Figure 3, the chains are interlinked along the [001] direction by the H-bond forming between atom O(8) of the oxalate group and atom H(1) of the $HAsO_4^{2-}$ group. The distances and angle involved are $d_{H(1)\cdots O(8)}$ = 1.85 Å, $d_{O(4)\cdots O(8)}$ = 2.82 Å, and ∠O(4)−H(1)···O(8) = 164.1°. As a consequence, a 3D hydrogen-bonded network with large tunnels enclosing two arrays of piperazinium cations is formed. Hydrogen bonds also exist between oxalate anions and piperazinium cations. Each of the organic cations connects to three oxalate groups belonging to three different chains on the *bc* plane.

A view of the infinite chains down to the *c* axis (Figure 3) gives a layered motif similar to the four-connected net in the well-known structure of $VOPO_4\cdot 2H_2O$,[10] which is a chemical precursor of a wide family of oxovanadium(IV) or -(V) derivatives.[15] The layers in $VOPO_4\cdot 2H_2O$ are cleaved by the two terminal water oxygens occuping an edge of VO_6 octahe-

(9) Leonowicz, M. E.; Johnson, J. W.; Brody, J. F.; Shannon, H. F.; Newsam, J. M. *J. Solid State Chem.* **1985**, *56*, 370.
(10) Tietze, H. R. *Aust. J. Chem.* **1981**, *34*, 2035.
(11) Selwood, P. W. *Magnetochemistry*; Interscience: New York, 1956.
(12) Sheldrick, G. M. *SADABS*; Siemens Analytical X-ray Instrument Division: Madison, WI, 1995.
(13) Brown, I. D.; Altermann, D. *Acta Crystallogr.* **1985**, *B41*, 244.
(14) Sheldrick, G. M. *SHELXTL Programs*, Version 5.1; Bruker AXS, 1998.
(15) (a) Bordes, E.; Courtine, P. *J. Chem. Soc., Chem. Commun.* **1985**, 294. (b) Hodnett, B. K. *Catal. Rev. Sci. Eng.* **1985**, *27*, 373.

Table 2. Atomic Coordinates and Thermal Parameters (Å^2) for **1** and **2**

atom	*x*/*a*	*y*/*b*	*z*/*c*	U_{eq}[a]	atom	*x*/*a*	*y*/*b*	*z*/*c*	U_{eq}[a]
				1					
V(1)	−0.5167(1)	0.3847(1)	−0.0041(1)	0.017(1)	O(9)	−0.4159(7)	0.7058(3)	−0.0364(3)	0.040(1)
As(1)	−0.0120(1)	0.3720(1)	0.0389(1)	0.017(1)	N(1)	−0.1674(7)	0.3393(4)	−0.2104(3)	0.033(1)
O(1)	−0.2145(5)	0.3982(3)	−0.0247(3)	0.025(1)	N(2)	0.1199(7)	0.2953(4)	−0.3499(3)	0.028(1)
O(2)	−0.0108(6)	0.2475(2)	0.0812(2)	0.024(1)	C(1)	−0.4382(7)	0.5570(4)	−0.1396(3)	0.021(1)
O(3)	0.1850(5)	0.4023(3)	−0.0265(3)	0.026(1)	C(2)	−0.4541(7)	0.6099(4)	−0.0448(3)	0.025(1)
O(4)	−0.0054(7)	0.4576(2)	0.1308(2)	0.034(1)	C(3)	0.0046(11)	0.4154(3)	−0.2290(3)	0.030(1)
O(5)	−0.5185(6)	0.3419(2)	0.0991(2)	0.026(1)	C(4)	0.1841(8)	0.3538(5)	−0.2657(4)	0.029(1)
O(6)	−0.4967(6)	0.4604(2)	−0.1431(2)	0.021(1)	C(5)	−0.0531(8)	0.2211(4)	−0.3313(4)	0.032(1)
O(7)	−0.5087(6)	0.5486(2)	0.0203(2)	0.023(1)	C(6)	−0.2313(9)	0.2822(5)	−0.2940(4)	0.035(1)
O(8)	−0.3725(6)	0.6121(3)	−0.2042(2)	0.033(1)					
				2					
V(1)	−0.5071(1)	0.3821(1)	−0.0002(1)	0.015(1)	O(9)	−0.4315(5)	0.7056(2)	−0.0388(2)	0.035(1)
P(1)	−0.0037(2)	0.3685(1)	0.0372(1)	0.016(1)	N(1)	−0.1574(7)	0.3385(3)	−0.2082(3)	0.028(1)
O(1)	−0.1966(5)	0.3943(3)	−0.0190(2)	0.021(1)	N(2)	0.1301(6)	0.2978(3)	−0.3514(2)	0.023(1)
O(2)	−0.0020(6)	0.2528(2)	0.0724(2)	0.021(1)	C(1)	−0.4392(6)	0.5532(3)	−0.1389(3)	0.018(1)
O(3)	0.1863(4)	0.3958(3)	−0.0204(2)	0.021(1)	C(2)	−0.4567(6)	0.6080(3)	−0.0453(3)	0.020(1)
O(4)	0.0052(7)	0.4442(2)	0.1238(2)	0.028(1)	C(3)	0.0187(11)	0.4146(3)	−0.2258(3)	0.028(1)
O(5)	−0.5067(6)	0.3450(2)	0.1048(2)	0.025(1)	C(4)	0.2021(8)	0.3552(4)	−0.2675(3)	0.028(1)
O(6)	−0.4885(6)	0.4554(2)	−0.1401(2)	0.019(1)	C(5)	−0.0470(7)	0.2232(4)	−0.3333(3)	0.028(1)
O(7)	−0.5023(6)	0.5462(2)	0.0210(2)	0.022(1)	C(6)	−0.2251(8)	0.2842(5)	−0.2922(4)	0.032(1)
O(8)	−0.3792(6)	0.6079(3)	−0.2051(2)	0.030(1)					

[a] U_{eq} is defined as one-third of the trace of the orthogonalized $\boldsymbol{U}_{ij}$ tensor.

Table 3. Selected Bond Lengths (Å) and Bond Valence Sums ($\sum s$) for **1** and **2**[a]

	1		
V(1)−O(1)	2.012(3)	V(1)−O(5)	1.603(3)
V(1)−O(2)a	1.998(3)	V(1)−O(6)	2.247(3)
V(1)−O(3)b	1.996(3)	V(1)−O(7)	2.075(3)
$\sum s$[V(1)−O] = 4.04			
As(1)−O(1)	1.655(3)	As(1)−O(3)	1.652(4)
As(1)−O(2)	1.671(3)	As(1)−O(4)	1.717(3)
$\sum s$[As(1)−O] = 5.15			
C(1)−C(2)	1.540(7)	C(1)−O(8)	1.246(6)
C(1)−O(6)	1.264(5)	C(2)-O(9)	1.229(6)
C(2)−O(7)	1.273(5)	N(1)−C(3)	1.500(8)
N(2)−C(4)	1.493(7)	N(2)−C(5)	1.489(7)
N(1)−C(6)	1.475(8)	C(3)−C(4)	1.505(8)
C(5)−C(6)	1.499(8)		
	2		
V(1)−O(1)	2.013(3)	V(1)−O(5)	1.607(2)
V(1)−O(2)a	1.989(2)	V(1)−O(6)	2.248(3)
V(1)−O(3)b	1.993(3)	V(1)−O(7)	2.070(2)
$\sum s$[V(1)−O] = 4.05			
P(1)−O(1)	1.519(3)	P(1)−O(3)	1.519(3)
P(1)−O(2)	1.533(2)	P(1)−O(4)	1.583(3)
$\sum s$[P(1)−O] = 4.97			
C(1)−C(2)	1.536(6)	O(6)−C(1)	1.260(4)
O(8)−C(1)	1.247(5)	O(7)−C(2)	1.275(5)
O(9)−C(2)	1.232(5)	N(1)−C(3)	1.496(7)
N(2)−C(4)	1.496(6)	N(2)−C(5)	1.490(6)
N(1)−C(6)	1.470(7)	C(3)−C(4)	1.517(8)
C(5)−C(6)	1.497(7)		

[a] Symmetry codes: (a) $x - {}^1/_2, -y + {}^1/_2, -z$; (b) $x - 1, y, z$.

dron, resulting in the infinite ladder-like chains in $VOHPO_4 \cdot 4H_2O$. Structural relationship of the title compounds to the parent $VOPO_4 \cdot 2H_2O$ is then obvious in that the oxalate anion plays the same role as terminal coordination water molecules. Oppositely, they provide bridges between inorganic chains or sheets to generate 3D open frameworks in the existing iron phosphatooxalates.[6,7]

Both of the title compounds are thermally stable to ca. 250 °C as indicated by the TG curves drawn in Figure 4. The weight loss of compound **1** can be divided into two stages. The first stage, which occurs from 250 to ∼380 °C, is attributed to the decomposition of oxalate anion and piperazinium cation (calcd

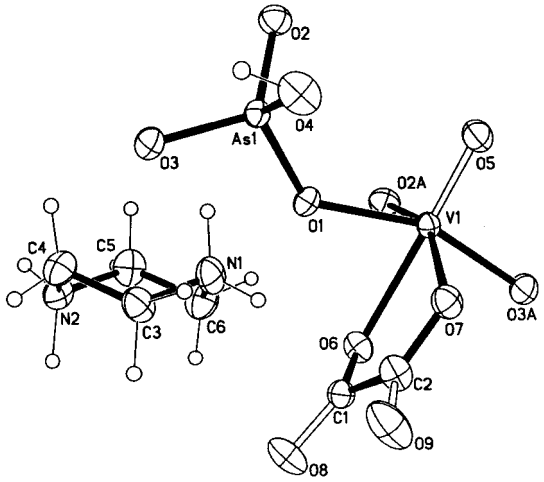

Figure 1. Atoms of the asymmetric unit of $(C_4H_{12}N_2)[VO(C_2O_4)HAsO_4]$ (**1**), showing the atom-labeling scheme and 50% thermal ellipsoids. Open bonds indicate the V═O groups.

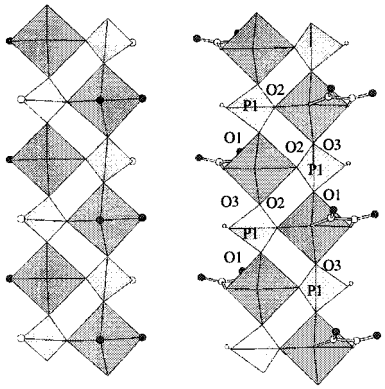

Figure 2. Section of the ladder-like chain in $(C_4H_{12}N_2)[VO(C_2O_4)HPO_4]$ (**2**) (right) and $VO(HPO_4) \cdot 4H_2O$ (left). Black dots in the plot of $VO(HPO_4) \cdot 4H_2O$ represent coordination water molecules.

45.5% for $2CO_2$ and $C_4H_{10}N_2$). The second stage occurs between temperatures of ∼380 and 700 °C which is due to dehydration of the thermal product and decomposition of the arsenate group (calcd 35.0 for $1{}^1/_2H_2O$, ${}^1/_4O_2$, and ${}^1/_2As_2O_3$). The observed total

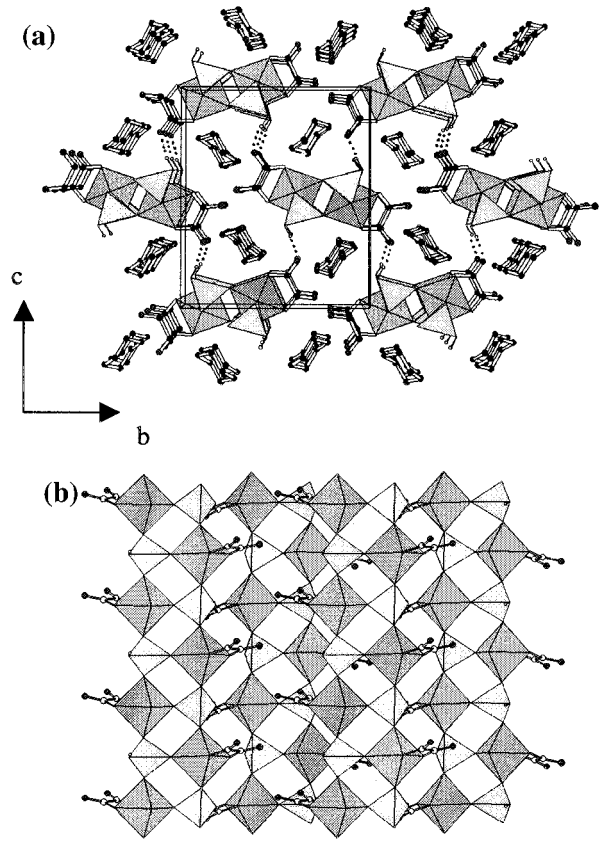

Figure 3. Polyhedral representations of $(C_4H_{12}N_2)[VO(C_2O_4)HAsO_4]$ (**1**). (a) A perspective view of the structure along the *a* axis. Dashed lines represent H bonds. (b) View of the structure along the *c* axis, showing the four-connected layer-like motif. In these representations, the darker polyhedra are VO_6 octahedra, the lighter ones are AsO_4 tetrahedra, large open circles are C atoms, small circles are H atoms, stippled circles are N atoms, and solid circles are O atoms.

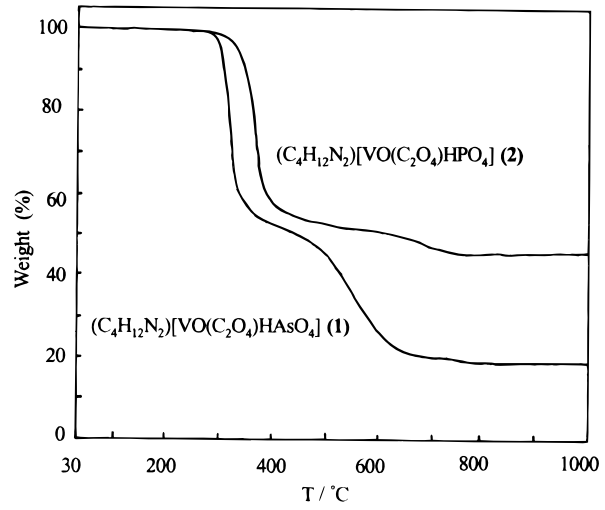

Figure 4. Thermogravimetric curves for $(C_4H_{12}N_2)[VO(C_2O_4)HAsO_4]$ (bottom) and $(C_4H_{12}N_2)[VO(C_2O_4)HPO_4]$ (up) in flowing N_2 at 10 °C min^{-1}.

weight loss (81.2%) of the two stages can be compared well with the calculated value of 80.5% based on the above interpretation. For compound **2**, the TG curve shows only one sharp fall of weight loss corresponding to the decomposition of oxalate anion, piperazinium cation and dehydration of HPO_4 group. The weight loss from 250 to ~370 °C should be attributed to the evolution of $2CO_2$ and $^1/_2H_2O$ (calcd 28.7%). A sequential weight loss that occurred in the region ~370−780 °C should correspond to the decomposition of piperazinium cation (calcd 25.4% for $C_4H_{10}N_2$). The same tailing which spans over a range of 400 °C for the release of the organic component has been observed in other piperazinium cation-containing metal phosphates[8,16] In total, the observed loss of 53.37% is in good agrement with the calculated value of 54.14% based on the above interpretation.

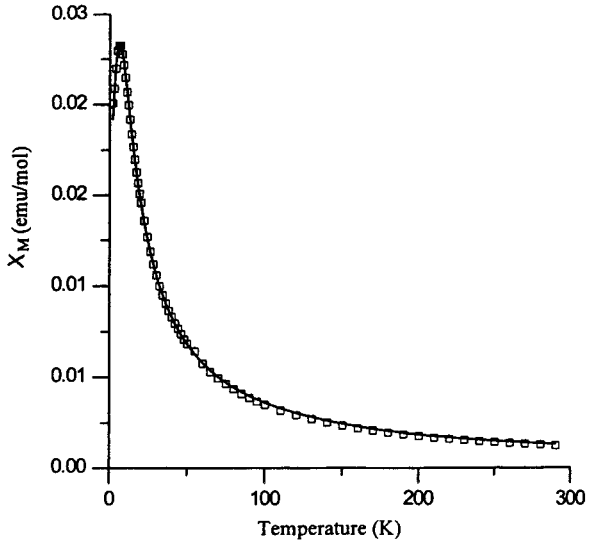

Figure 5. Molar magnetic susceptibility (χ_M) vs *T* curve in the range 2−300 K for $(C_4H_{12}N_2)[VO(C_2O_4)HPO_4]$ (**2**).

Figure 5 exhibits the temperature-dependent molar magnetic susceptibility of the compound **2** in the range 2−300 K. At 300 K the magnetic moment (μ_{eff}) per formula, determined from the equation $\mu_{eff} = 2.828(\chi_M T)^{1/2}$, is 1.67 μB which is slightly lower than that expected for an isolated paramagnetic system with $S = {}^1/_2$ ($\mu_{eff} = 1.73$ μB). Upon cooling, χ_M increases and reaches a maximum at about 6 K, indicating a weak antiferromagnetic interaction. This antiferromagnetic character is further suggested by a small negative Weiss constant ($\theta = -2.2$ K) determined in the temperature range 80−300 K.

Since the structure of the title compounds is a one-dimensional ladder-like motif. Two pathways are possible in mediating the magnetic coupling between the VO^{2+} centers: one is through O(3)−P(1)−O(2) and the other is through O(3)−P(1)−O(1) (refer to Figure 2). Considering that the V(1)···V(1) distances is 4.60 Å through the first pathway which is significantly shorter than that through the second pathway (6.41 Å), the antiferromagnetic interaction could be mainly attributed to the exchange couplings between the vanadyl ions through O(3)−P(1)−O(2) atoms. The susceptibility data were therefore analyzed by using an equally spaced chain model for spin $S = {}^1/_2$ with the expression $\chi_M = (Ng^2\mu_B^2/kT)(0.25 + 0.14995x + 0.30094x^2) \times (1 + 1.9862x + 0.68854x^2 + 6.0626x^3)^{-1}$, where *N*, *g*, μ_B, and *k* have their usual meanings and $x = |J|/kT$. *J* is the coupling constant between the neighboring vanadyl ions. A good fit was obtained which affords the solid line in Figure 5 with $g = 1.97$, $J = -2.85$ cm^{-1} and the coefficient of determination (r^2) is 0.99974. The χ_M vs *T* plot of compound **2** is very similar to that of compound **1**. A good fit of the magnetic data was also obtained using the same Bonner and Fisher $S = {}^1/_2$ linear−chain model[17] with $g = 1.97$, $J = -1.88$ cm^{-1} and $r^2 = 0.99951$.

(16) Structures of $(C_6H_{14}N_2)_3[(MoO_2)_4(C_2O_4)_4(H_2PO_4)_2]\cdot 8.5H_2O$, $(C_4H_{12}N_2)[MoO_2(H_2AsO_4)(AsO_4)]$, and $(C_4H_{12}N_2)[MoO_2(C_2O_4)(HAsO_4)]$ are to be submitted.

(17) Bonner, J.; Fisher, M. E. *Phys. Rev., Sect. A* **1964**, *135*, 640.

In conclusion, we have successfully prepared two vanadyl(IV) arsenato- and phosphato-oxalates using piperazine as a templating agent. They are the first inorganic−organic mixed anion materials in the vanadium arsenate and vanadium phosphate systems. The ladder-like chain structure can be considered as an organic derivative of $VOHPO_4 \cdot 4H_2O$ or $VOPO_4 \cdot 2H_2O$. Magnetic study showed exchange coupling may occur between the nearest VO^{2+} centers along the infinite chains. In contrast to the existing iron phosphatooxalates in which the oxalate groups bridge chains or sheets to generate 3D frameoworks, this work shows that the incorporation of oxalate anions into inorganic anions can as well result in structures of lower dimensionality. Additional examples of the latter case has also been observed in the Mo^{VI}/As/O system.[16]

Acknowledgment. We are grateful to the National Science Council of the Republic of China for support of this work. We also thank Prof. Limin Zheng at State Key Laboratory of Coordination Chemistry, Nanjing University, for discussion in the magnetic study.

Supporting Information Available: X-ray crystallographic data including tables of complete crystal data, atomic coordinates, bond distances and angles, and anisotropic thermal parameters for **1** and **2**. This material is available free of charge via the Internet at http://pubs.acs.org.

IC990501P